Effect of oxygen agglomeration in polycrystalline Si (SIPOS) films

I. P. LISOVSKYY, V. G. LITOVCHENKO, B. M. GNENYY
Institute of Semiconductor Physics, 41 Nauky prosp., Kyev-28, 252028, Ukraine

W. FUSSEL
Hahn-Meitner Institute, Berlin 0-1199, Germany

A. E. KIV, V. N. SOLOVIEV, T. I. MAXIMOVA
Ben-Gurion University, Department of Material Engineering, P.O. Box. 653, Beer-Sheva, 84105, Israel
E-mail: kiv@bgumail.bgu.ac.il

IR transmission spectra of SIPOS structures were measured and were investigated by using an approach of deconvolution of the Si–O stretching band into Gauss profiles. It was found that the space distribution of oxygen in SIPOS layers treated at elevated temperatures does not correspond to the prediction of RBM statistics. The oxygen agglomeration was observed. Optical microscopy was also applied to get additional information about the SIPOS films after treatment in HF solution. The peculiarities of the space distribution of oxygen in SIPOS films are explained on the basis of a computer simulation of free Si surface relaxation. A computer model has shown that a disordered phase arises in the Si surface layers at elevated temperatures. This phase is characterized by a large concentration of stressed and dangling bonds. There are lattice nodes with more than one dangling bond that are suitable sites for oxygen agglomeration.
© *2002 Kluwer Academic Publishers*

1. Introduction
Semi-insulating polycrystalline oxygen-doped silicon (SIPOS) layers are widely used in the technology of high-voltage devices, of silicon solar cells and of special transistor structures [1–3]. There are good prospects for further applications of these materials. Nowadays it is established that a concentration and a structural arrangement of oxygen atoms essentially affect optical, chemical, and electrical properties of SIPOS films. It was found that in polycrystalline silicon annealed at temperatures of 600–1000 °C the electrically active donors linked to oxygen precipitates were formed [4, 5]. This is why the important aim is to obtain information about the space distribution of oxygen and about the nature of chemical bonds in SIPOS structures.

It is known that bridging oxygen (in Si–O–Si "molecules") reveals itself in infrared absorption spectrum as an absorption peak in the range 1000–1100 cm^{-1}. It was shown [6–8] that by a deconvolution of the Si–O stretching band into elementary profiles and by analyzing their positions and intensities one can obtain parameters of short-range and local order in SiO_X films. In this work we applied this approach to investigate SIPOS structures.

Recently it was established that a high-temperature treatment $(T > 600 °C)$ of silicon leads to the formation of a quasi-disordered phase (QDP) in surface layers

[9, 10]. QDP is characterized by specific features of electronic and atomic structures. The main peculiarities of QDP are the non-saturated and stressed bonds non-uniformly distributed in several Si surface layers.

So far, as in polycrystalline silicon, the main properties are determined by surface layers and it is clear that QDP plays an important role in the formation of SIPOS structures.

The paper consists of two parts. In the first part the experimental procedure and results linked to space distribution of oxygen in SIPOS layers are described. In the second part we have explained experimental results from computer simulation of silicon surface layers.

2. Experimental procedure and results
SIPOS layers were deposited at 620 °C on Si wafers by a chemical vapor deposition (CVD) technique. A mixture of N_2O and SiH_4 with the concentration ratio in the limits from 0 to 1 was used. The oxygen content was measured by the Rutherford backscattering technique. The concentration of oxygen (C_o) was changed from 0 up to 48 at %. The investigated SIPOS films were in the thickness interval from 90 to 460 nm. The IR transmission spectra were measured in the range 900–1300 cm^{-1}.
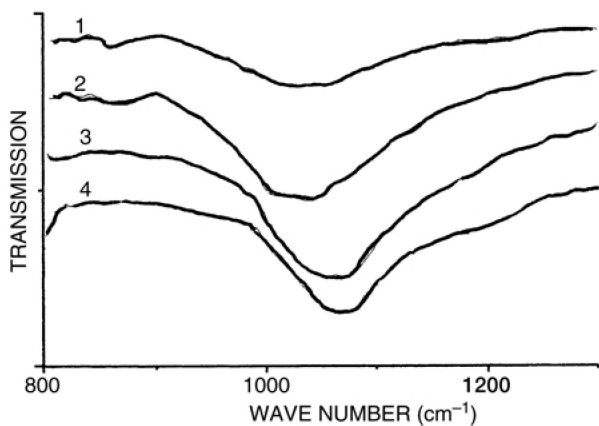
Figure 1 IR transmission spectra (in relative units) for SIPOS films with different oxygen content. Curves 1, 2, 3 and 4 correspond to oxygen concentration of 6.5, 12.7, 30.7 and 42.7 at %, respectively.

Deconvolution of the IR absorbance curves into the Gauss profiles was performed and the main contributions to the absorption spectra were separated. The details of the deconvolution procedure are described in Lisovskii *et al.* [6]. To obtain unambiguous data the results of deconvolution were analyzed for many shapes of absorbance curves. The deconvolution accuracy was estimated by a comparison of the summed Gauss profiles and the experimental ones using the least squares method. The deviation did not exceed 5×10^{-2}.

The IR transmission spectra of SIPOS samples were measured before and after the heat treatment and for various oxygen contents. We studied the main characteristics of the elementary profiles, such as the maximum position, the linewidth and the area under the elementary curve. Optical microscopy was also applied to get additional information about the SIPOS layers after their treatment in HF solution.

Fig. 1 shows the absorbance spectra of some investigated samples. It is seen that the maximum position and the band area depend on the oxygen content. As C_o increased the peak position shifted to larger wave numbers. In the case shown in Fig. 1, this shift is from $1040 \, \text{cm}^{-1}$ (for $C_o = 6.5 \, \text{at} \%$ to $1065 \, \text{cm}^{-1}$ (for $C_o = 42.7 \, \text{at} \%$). The band area increased by ~3.5 times for the same samples. Analogous effect was observed for SiO_X films in Lehmann *et al.* [11] and Gazorzewski *et al.* [12].

After the heat treatment (900 °C, 1 h inert ambient) the peak position became approximately the same $(1080 \, \text{cm}^{-1})$ for all investigated SIPOS films, but the band areas remained practically unchanged. In the case of the oblique light incidence the distortion of the spectrum shape took place for the samples with rather high oxygen content. This effect observed for SiO_X films [11] was explained by LO-TO splitting.

In Fig. 2 the deconvolution of an IR absorbance curve into Gauss profiles is shown. The parameters of the contributions for different Gauss profiles are given in Table I.

It should be noted that the separated profiles were present in all spectra independent of the spectrum shape, which sometimes changed drastically as a result of film annealing or variation of the angles of light incidence.

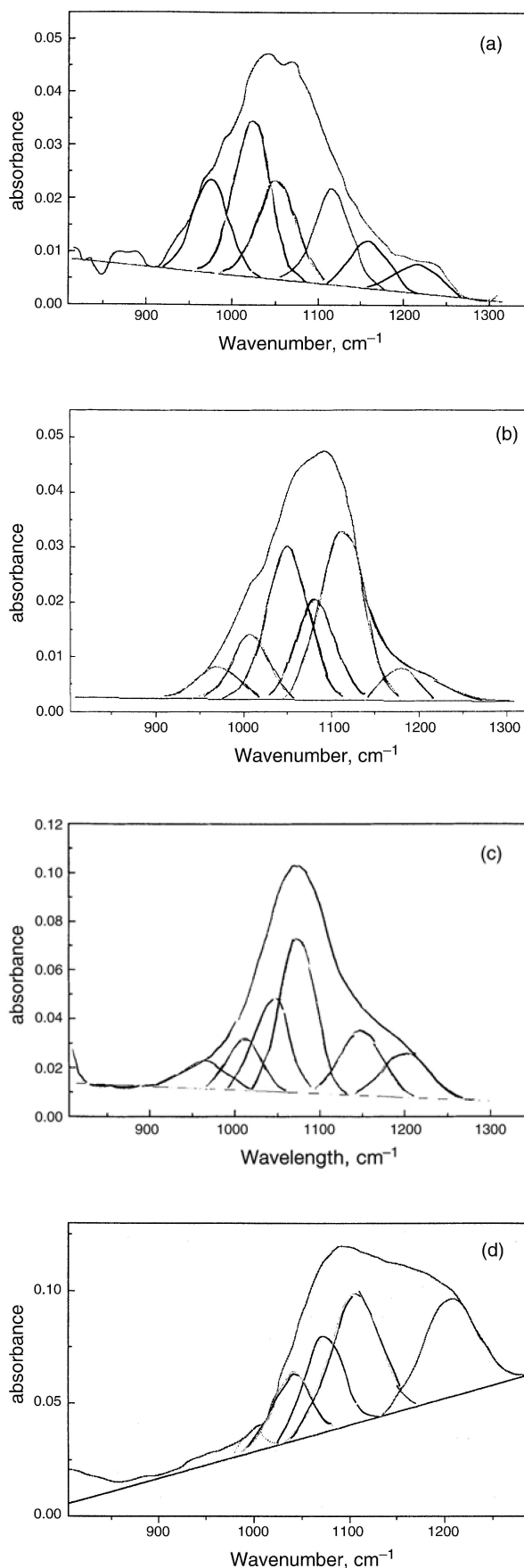One can see that the Si–O stretching band of SIPOS

Figure 2 Deconvolution of the main absorption band for SIPOS films into Gauss profiles (a, c, d – initial samples b – annealed one). Oxygen content: a, b – 6.5 at %; c, d – 47.7 at %. Spectra were measured at normal (a, b, c) and oblique (d) light incidence.

layers can be mainly represented as the sum of four elementary transverse absorption bands. Their number, maximum positions and full width at half peak maximum

Contribution	Maximum position, cm^{-1}	FWHM	Mode	Si–O–Si bond angle (°)	Molecular complex
X1	1001 ± 2	50 ± 2	TO	116	$Si-O-Si_3$
X2	1033 ± 1	45 ± 2	TO	127	$Si-O_2-Si_2$
X3	1067 ± 2	50 ± 2	TO	136	$Si-O_3-Si$
X4	1096 ± 4	55 ± 1	TO	145	$Si-O_4$
X5	1141 ± 2	56 ± 1	LO	114	$Si-O-Si_3$
X6	1195 ± 3	60 ± 5	LO	124	$Si-O_2-Si_2$
X7	1246 ± 2	50 ± 1	LO	140	$Si-O_4$

(FWHM) are the same as in the case of SiO_X amorphous films [6, 7], and therefore, the nature of the elementary profiles is also the same as in the case of the mentioned amorphous structures. This means that the components of the structure of SIPOS layers are $Si-O_Y-Si_{4-Y}$ clusters with $0 \leq y \leq 4$ (see Table I).

Sometimes the band maximum position (BMP) is used to determine the oxygen concentration in SiO_X films. However, analysis of the results obtained in a set of studies [13–18] shows that the correlation between the BMP and C_0 is ambiguous and depends on the process of film preparation. Moreover, annealing of such layers in the inert ambient resulted in a shift of BMP [13].

In our experiments it was observed that the BMP became practically the same ($1080 \, cm^{-1}$) for all annealed films regardless of oxygen content. These results indicate that the BMP does not correlate with oxygen concentration. This parameter is most probably connected with film microstructure.

Using the results of deconvolution and taking into account that only the band area is directly connected with the oxygen concentration one can estimate the contribu-

tion of each kind of molecular silicon-oxygen cluster to the film network. In fact, areas of the elementary bands X1–X4 (S_Y) are proportional to the concentrations of the bridging oxygen incorporated into complexes $Si-O_Y-Si_{4-Y}$ with $Y = 1, 2, 3, 4$, respectively [8]. Fig. 3 shows the dependences of S_Y/S_O on x (where S_O is the sum of X1–X4 profiles areas, i.e. the area of the transverse absorption mode, and x is the portion of corresponding structures).

Solid lines in Fig. 3 represent the probabilities of the oxygen bridges existing in molecular clusters $Si-O_Y-Si_{4-Y}$, which are calculated on the basis of the RBM statistics [8, 11]. Fig. 3a and b correspond to initial and to heat-treated samples, respectively. We see that the concentrations of $Si-O-Si_3$ and $Si-O_2-Si_2$ clusters are smaller, and the concentrations of $Si-O_3-Si$ and $Si-O_4$ clusters are sufficiently larger than those predicted by RBM statistics.

In Fig. 4 the micrographs of surfaces of the initial SIPOS layers and of layers that were treated in HF solution are presented. It may be seen that such treatment of specimens results in the occurrence of wells and pinholes. Since silicon and silicon oxides with low oxygen
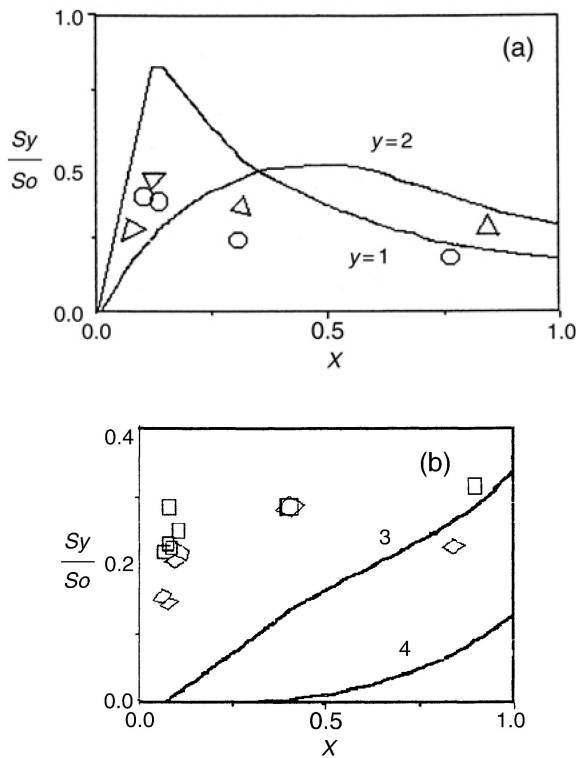

Figure 3 Contribution of bridging oxygen in different molecular complexes $Si-O_y-Si_{4-y}$ ($y = 1$ (circles), $y = 2$ (triangles), $y = 3$ (squares), $y = 4$ (rhombus)) in investigated films. Solid lines represent the probability of existence of the corresponding oxygen bridges, which was calculated in the framework of RBM statistics.
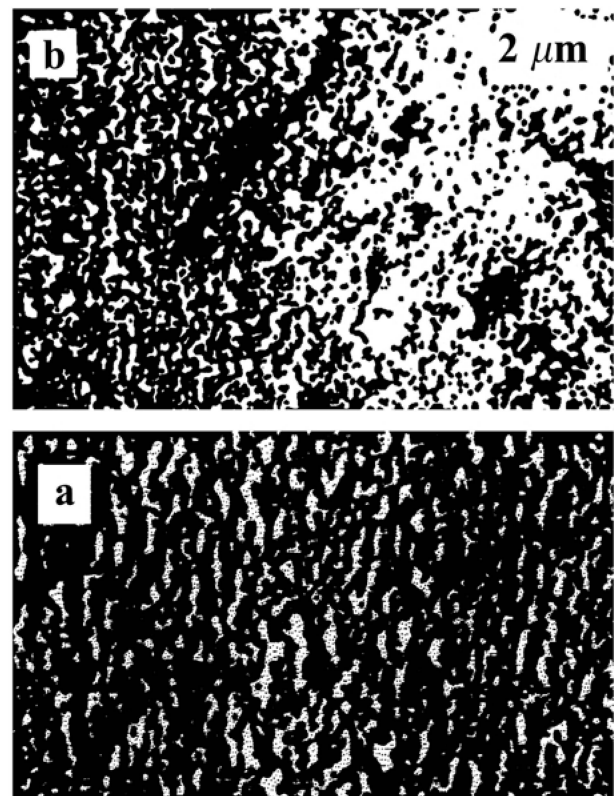

Figure 4 Micrographs of the surfaces of (a) the initial (b) and etched during 2 h in 20% HF solution SIPOS films.

169

content are practically insensitive to HF, one can assume that the wells observed are connected with removal of inclusions SiO_X with $X > 2$. The Si–O stretching bands for the etched samples have lesser contribution of the Gauss profiles with maximum positions 1067 and $1096\,cm^{-1}$ (see Fig. 5), which means that such layers have the structure with reduced contributions of $Si-O_3-Si$ and SiO_4 clusters.

3. Model of oxygen agglomeration in SIPOS structures

For polycrystalline materials, atomic and electronic structures of the grain boundaries play a dominant role in the progress of solid-state quasi-chemical reactions at high temperatures (oxidation, chemical adsorption, etc.). To explain the experimental results we performed molecular dynamics (MD) simulation of the micro-structure of Si surface layers relaxed at temperatures 600–1000 K by analogy to Jacobs et al. [19]. The main attention was paid to the space distribution of non-saturated chemical bonds. The starting configuration was taken as a parallelepiped containing 864 atoms: 12 layers with 72 atoms in each one. Periodic boundary conditions were used in two dimensions. The lower layer was fixed. The MD method was used in its standard form [19] with the Stillinger–Weber potential [20]. The time step was $10^{-14}\,s$.

To investigate the full relaxation of Si surface layers a new approach to MD simulation was applied. An algorithm of calculations included a procedure of rebuilding and rehybridization of chemical bonds. By analogy to [19] in the relaxation process any atom had a possibility to change its neighboring atoms and may form new chemical bonds.

We investigated in detail the QDP in Si surface layers relaxed at temperatures 900–1000 K. In this condition as a rule four or five surface layers belong to QDP. The non-usual polygons with the number of angles $n = 3–9$ and nodes with 1–3 dangling bonds may be seen in Figs 6 and 7.

Radial distribution functions (RDF) and angle distribution functions (ADF) in the range of QDP spectra are similar to those in a-Si, as may be seen in Fig. 8 (ADF are the angles between chemical bonds).
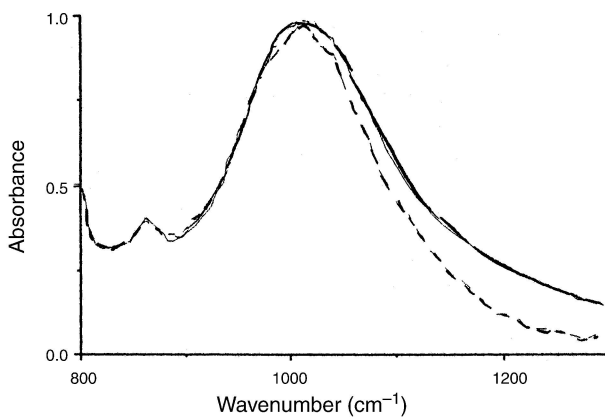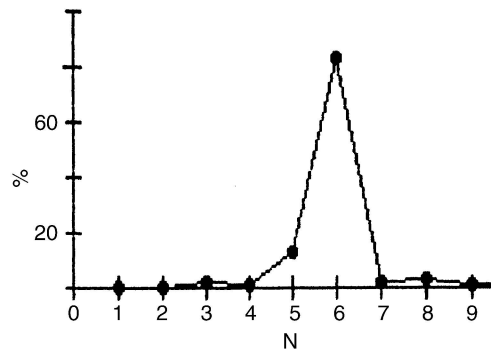

Figure 6 Distribution of polygons with different number (N) of angles in QDP of Si surface layers.
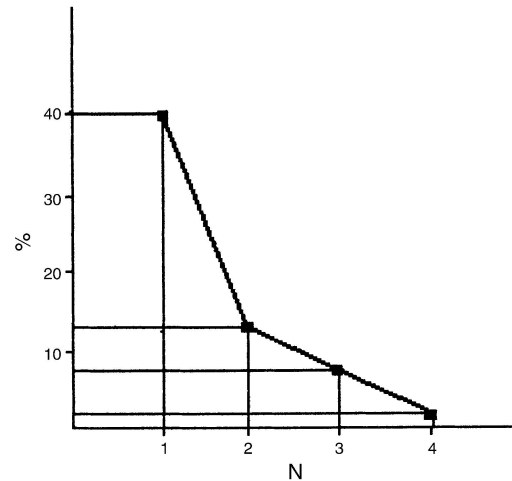

Figure 7 Distribution of atoms in QDP with $n = 1–4$ dangling bonds. Atoms with four dangling bonds are interstitial ones.
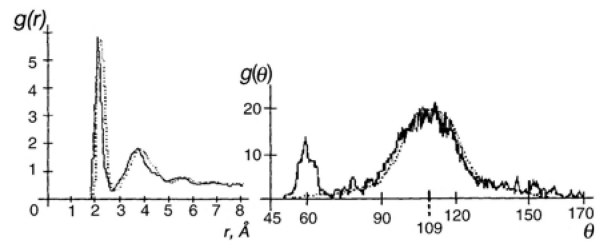

Figure 8 Radial distribution functions (left) and angle distribution functions for angles between chemical bonds (right) in relaxed surface layers of silicon. Dotted lines correspond to a-Si.

Simulation results have shown that each of the surface layers that form QDP has specific microstructure characteristics. For example, only the third layer has no nodes with more than one dangling bond and at the same time this layer is the most distorted one.

The main experimental result that was obtained in this work is a deviation of the oxygen distribution over SiO_X structures in SIPOS films from the usual ones that RBM statistics predicts [8]. At the temperatures of SIPOS film deposition the surface layers of each grain form QDP. So the Si–O interactions and the space distribution of oxygen in SIPOS films are determined by peculiarities of QDP.

The nodes with more than one dangling bond are the favorable sites for SiO_X structures with large oxygen content formation. The comparison of Si–O–Si bond

Figure 5 Absorbance spectra (in relative units) for initial (solid line) and etched (dashed line) SIPOS layers.

angles in Table I and in Fig. 8 shows that in the region of $136°–145°$ we have a considerable concentration of molecular complexes Si–O$_3$–Si and Si–O$_4$.

We have seen that the QDP is located in several surface layers where we may observe the microregions with strongly oxidized silicon in the network of SIPOS films. The results presented in Figs 4 and 5 show that the samples with etched surface layers (HF treatment) have a decreased content of oxygen and this is also in agreement with the QDP model.

4. Conclusion

By using IR spectroscopy SIPOS films were investigated. New possibilities to obtain the distribution of oxygen over the Si–O clusters were demonstrated by using a method of deconvolution of Si–O IR spectra stretching band into the elementary Gauss profiles. This approach allows one to clarify the main structural elements in the network of SIPOS layers. It was established that the high-temperature treatment of SIPOS films leads to increasing the concentration of SiO$_X$ clusters with a large content of oxygen $(X = 3, 4)$. The effect of oxygen agglomeration in SIPOS films is explained by results of MD simulation of high-temperature relaxation of Si surface layers. In conditions of full relaxation of Si surface layers at elevated temperatures the QDP arises, which is characterized by a high concentration of dangling and stressed bonds and by deviations of angles between chemical bonds from their normal values in tetrahedral structures. The peculiarities of QDP in Si surface layers can explain the main experimental results concerning the oxygen agglomeration in SIPOS films.

References

1. P. AKHTER, M. N. ZAKIR, A. BAIG, *Semicond. Sci. Technology* **6** (1991) 135.
2. C. J. VALKER, J. D. WHITFIELD and P. L. FEJES, *Mater. Res. Soc. Symp. Proc.* **14** (1983) 187.
3. K. NAUKA, H. C. GATOS and J. LAGOVSKY, *Appl. Phys. Lett.* **43** (1983) 241.
4. J. PARK, M. DUECHER and H. J. MOELLER, in "Proceedings of the Twelfth European Photovoltaic Solar Energy Conference, Amsterdam, June 1994", edited by J. Park (Elsevier Science, Kidlington, 1994) p. 996.
5. I. E. REIS, J. CHUNG and H. J. MOELER, in "Proceedings of the Eleventh European Photovoltaic Solar Energy Conference Montreux September 1992" edited by J. Park (Elsevier Science, Kidlington, 1992) p. 499.
6. I. P. LISOVSKII, V. G. LITOVCHENKO, V. B. LOZINSKII and G. I. STEBLOVSKII, *Thin Solid Films* **213** (1992) 164.
7. I. P. LISOVSKII, V. G. LITOVCHENKO, V. B. LOZINSKII, V. P. MELNIK and S. I. FROLOV, *ibid.* **247** (1994) 264.
8. I. P. LISOVSKII, V. G. LITOVCHENKO, V. B. LOZINSKII, S. I. FROLOV, H. FLIETNER, W. FUSSEL and E. SCHMIDT, *J. Non-Cryst. Solids* **87** (1995) 91.
9. A. E. KIV, V. N. SOLOVIEV and T. I. MAXIMOVA, *Semicond. Phys., Quantum Electron. Optoelectron.* **3** (2000) 157.
10. H. HIBINO, K. SUMITOMO and T. FUKUDA, *Phys. Rev. B* **58** (1999) 12587.
11. A. LEHMANN, L. SCHUMANN and K. HUBNER, *Phys. Status Solid B* **121** (1984) 505.
12. P. GAWORZEWSKI, E. HILD, F.-G. KIRSCHT and L. VECSERNYES, *Phys. Status Solid A* **85** (1984) 133.
13. M. NAKAMURA, Y. MOCHIZUKI, K. USAMI, Y. ITOH and T. NOZAKI, *Solid State Commun.* **50** (1984) 1079.
14. I. P. LISOVSKYY, V. G. LITOVCHENKO, B. M. GNENYY, D. O. MAZUROV, W. FUSSEL, A. E. KIV, T. I. MAXIMOVA and V. N. SOLOVIEV, *Phys. Low-Dim. Struct.* **7/8** (2001) 113.
15. A. P. DOSTANKO, E. S. AKULICH, V. YA. SHIRIPOV and S. A. SOBOLEV, *J. Appl. Spectrose* **50** (1989) 436.
16. I. V. SVADKOVSKII, E. S. AKULICH, V. YA. SHIRIPOV and A. P. DOSTANKO, *ibid.* **55** (1991) 322.
17. G. V. SIDORENKO, N. N. SYRBU, A. T. GAPONENKO and V. D. PRILEPOV, *Elektronnaya Tekhnika, Seria Materialy* **256** (1991) 49.
18. W. FUSSEL, W. HENRION and R. SCHOLZ, *Microelectr. Eng.* **22** (1993) 355.
19. P. W. JACOBS, A. E. KIV, R. M. BALABAY, N. V. GRISCHENKO, V. V. CHISLOV, I. I. DONCHEV and S. V. PRIKHODNAYA, *Comput. Model. New Technol.* **2** (1998) 15.
20. F. H. STILLINGER and T. A. WEBER, *Phys. Rev. B* **31** (1985) 52.
21. F. F. ABRAHAM and I. P. BATRA, *Surf. Sci.* **163** (1985) L752.